

## 1 **Methylation pattern of *nc886* in non-human mammals**

2 Daria Kostiniuk<sup>1¥</sup>, Hely Tamminen<sup>1¥</sup>, Pashupati P. Mishra<sup>2</sup>, Saara Marttila<sup>1,3#</sup> Emma  
3 Raitoharju<sup>1#\*</sup>

4 <sup>1</sup>Molecular Epidemiology, Faculty of Medicine and Health Technology, Tampere University,  
5 Tampere, Finland

6 <sup>2</sup>Department of Clinical Chemistry, Pirkanmaa Hospital District, Fimlab Laboratories, and  
7 Finnish Cardiovascular Research Center, Tampere, Faculty of Medicine and Health  
8 Technology, Tampere University, Tampere, Finland

9 <sup>3</sup>Gerontology Research Center, Tampere University, Finland

10 <sup>¥</sup> and <sup>#</sup> Equal contribution

11 **\*Corresponding Author:** Emma Raitoharju, PhD, Molecular Epidemiology, Tampere  
12 University, Tampere, Finland. Tel: +358 50 318 7676.

13 Email: emma.raitoharju@tuni.fi

14

15 **Abstract**

16 **Background:** In humans, the *nc886* locus is a polymorphically imprinted metastable epiallele.  
17 Periconceptual conditions have an effect on the methylation status of *nc886*, and further, this  
18 methylation status is associated with health outcomes in later life, in line with the  
19 Developmental Origins of Health and Disease (DOHaD) hypothesis. Animal models would  
20 offer opportunities to study the associations between periconceptual conditions, *nc886*  
21 methylation status and metabolic phenotypes further. Thus, we set out to investigate the  
22 methylation pattern of the *nc886* locus in non-human mammals.

23 **Data:** We obtained DNA methylation data from the data repository GEO for mammals, whose  
24 *nc886* gene included all three major parts of *nc886* and had sequence similarity of over 80%  
25 with the human *nc886*. Our final sample set consisted of DNA methylation data from humans,  
26 chimpanzees, bonobos, gorillas, orangutangs, baboons, macaques, vervets, marmosets and  
27 guinea pigs.

28 **Results:** In human data sets the methylation pattern of *nc886* locus followed the expected  
29 bimodal distribution, indicative of polymorphic imprinting. In great apes, we identified a  
30 unimodal DNA methylation pattern with 50% methylation level in all individuals and in all  
31 subspecies. In Old World monkeys, the between individual variation was greater and  
32 methylation on average was close to 60%. In guinea pigs the region around the *nc886*  
33 homologue was non-methylated. Results obtained from the sequence comparison of the CTCF  
34 binding sites flanking the *nc886* gene support the results on the DNA methylation data.

35 **Conclusions:** Our results indicate that unlike in humans, *nc886* is not a polymorphically  
36 imprinted metastable epiallele in non-human primates or in guinea pigs, thus implying that  
37 animal models are not applicable for *nc886* research. The obtained data suggests that the *nc886*

38 region may be classically imprinted in great apes, and potentially also in Old World monkeys,  
39 but not in guinea pigs.

40

41 **Key words:** nc886, vtRNA2-1, primates, imprinting, DNA methylation

42

## 43 **Background**

44 In mammalian genomic imprinting, only one parental allele is expressed, while gene expression  
45 from the other allele is suppressed in a parent-of-origin-dependent manner. The expression of  
46 imprinted genes in general has been associated with fetal and placental growth and suggested  
47 to have a role in the development of cardiometabolic diseases in adulthood [1–3]. Imprinting  
48 arose relatively recently at most loci— while only a few imprinted genes in Eutherians are also  
49 imprinted in marsupials, to date no imprinting has been reported in the egg-laying monotreme  
50 mammals [4]. Genetic imprinting is best described in mice, and while the mouse is an  
51 informative proxy for human imprinted gene regulation, less than half of the 100 human  
52 imprinted genes have been shown to be similarly imprinted in mice  
53 (<https://www.geneimprint.com/site/home>). Distinct differences in placental evolution,  
54 physiology, and reproductive biology of the primate and murine groups may be responsible for  
55 these differences.

56 During gametogenesis and fertilization, the original DNA methylation pattern of imprinted  
57 genes is erased, and parent of origin-based methylation pattern is established. While most  
58 imprinted genes are located in clusters that are regulated by insulators or long noncoding RNAs  
59 [5], some unclustered imprinted genes can be regulated by differential promoter methylation  
60 [3]. Parental imprints are maintained after fertilization through these mechanisms despite  
61 extensive reprogramming of the mammalian genome [3]. A common feature of imprinted genes  
62 is insulators, such as CCCTC binding factor (CTCF) binding sites, which block the enhancers  
63 from interacting with gene promoters and/or act as barrier to the spread of transcriptionally  
64 repressive condensed chromatin [6].

65 Due to the important developmental roles of the imprinted genes, imprinting is tightly fixed  
66 across human populations, with all individuals displaying monoallelic expression of imprinted

67 genes. An exception to this is the *non-coding 886* (*nc886*, also known as *VTRNA2-1*), which is  
68 the only polymorphically imprinted metastable epiallele that has been repeatedly described in  
69 humans in the literature. Non-coding RNA 886 is encoded in chromosome 5q31.1, from a 1.9-  
70 kb long, differentially methylated region (DMR), the boundaries of which are marked by two  
71 CTCF binding sites [7,8]. This DMR has been shown to present maternal imprinting in ~75%  
72 of individuals in several populations [7,9,10]. This means that while in all individuals the  
73 paternal allele is unmethylated, in approximately 75% of individuals the maternal allele is  
74 methylated (individuals present a 50% methylation level at *nc886* locus and are hemi-  
75 methylated) and in the remaining 25% of individuals the maternal allele is unmethylated  
76 (individuals present a 0% methylation level at the *nc886* locus and are non-methylated).

77 The *nc886* gene codes for a 102nt long, non-coding RNA, which is then cleaved into two short  
78 RNAs (hsa-miR-886-3p/*nc886*-3p [23 nt] and hsa-miR-886-5p/*nc886*-5p [24–25 nt]) [11–13].  
79 There is no consensus on whether the effects of *nc886* expression is mediated by the 102 nt  
80 long hairpin structure or the *nc886*-3p and -5p molecules, as the short molecules have been  
81 indicated to function as miRNAs, while the hairpin loop has been shown to inhibit protein  
82 kinase R (PKR) [11,14].

83 The periconceptional environment has been suggested to affect DNA methylation patterns in  
84 maternal alleles[15], including the *nc886* epiallele [7,8,10]. Season of conception, maternal age  
85 and socioeconomic status have been linked to changes in the proportion of non- and hemi-  
86 methylated offspring [7,8,10]. On the other hand, lower levels of *nc886* methylation have been  
87 linked to cleft palate [16], and a non-methylated *nc886* epiallele has been associated with an  
88 elevated childhood BMI [17]. The methylation status of this epiallele has also been associated  
89 with allergies [18], asthma [19], infections [20], and inflammation [21]. We and others have  
90 also shown that both the *nc886* methylation status and RNA expression are associated with  
91 indicators of glucose metabolism [10,22].

92 These results indicate that *nc886* could mediate the association between periconceptual  
93 conditions and later metabolic health, in line with the Developmental Origins of Health and  
94 Disease (DOHaD) hypothesis (aka the Barker hypothesis) [23]. More detailed analysis on  
95 periconceptual conditions and *nc886* methylation status and investigations between *nc886*  
96 and metabolic phenotypes, with less confounding factors, would be needed to confirm this  
97 hypothesis. As carcinogenesis [24] and pluripotency induction [10] affect the DNA  
98 methylation pattern in *nc886* locus, *in vitro* work has its limitations. Animal models could be  
99 a feasible option for this research. Unfortunately, rodents do not harbor the *nc886* gene, limiting  
100 the use of traditional model organisms [7]. Thus, this study was set up to investigate 1) which  
101 animals have *nc886* gene, 2) whether this gene is surrounded by similar CTCF elements as the  
102 human homolog and 3) whether the methylation status of the *nc886* region suggest  
103 polymorphic imprinting in non-human mammals.

## 104 **Materials and methods**

105 The presence of *nc886* gene was investigated in ensemble, in 65 amniota vertebrates Mercator-  
106 Pecan collection and 24 primates EPO-extended collection [25]. To select species for further  
107 investigation, we required the *nc886* gene have 80% sequence similarity with the human  
108 homolog and to present the sequences for *nc886-3p* and *nc886-5p* RNAs, as well as the loop  
109 structure, previously shown to mediate the binding of PKR [11,26] (Supplementary figures S1  
110 and S2). The existence and sequence similarity of the centromeric (chr5:135415115-  
111 135415544) and telomeric CTCF (chr5:135418124-135418523) binding site flanking *nc886*  
112 gene were also investigated in species shown to harbor intact *nc886* gene. If homologous  
113 CTCF-binding sites were not discovered, CTCFBSDB 2.0 [27] was utilized to predict possible  
114 non-homologous sites. Interactions of the *nc886* flanking CTCF-sites were also investigated  
115 using K562 CTCF CiA-PET Interactions data in genome browser [28].

116 For species harboring the *nc886* gene, we investigated the Gene Expression Omnibus (GEO)  
117 repository [29] for available DNA methylation data, with both general and binomial name of  
118 the species. DNA methylation data was available in apes from chimpanzees (*Pan troglodytes*,  
119 n=83; GSE136296 [30] and n=5; GSE41782 [31]), bonobos (*Pan paniscus*, n=6; GSE41782  
120 [31]), gorillas (*Troglodytes gorilla*, n=6; GSE41782 [31]) and orangutangs (*Pongo spp.*, n=6;  
121 GSE41782[31]). In Old World monkeys, data was obtained from baboons (*Papio spp.* n=28;  
122 GSE103287 [32]), rhesus macaques (*Macaca mulatta*, n=10; GSE103287 [32]), vervets  
123 (*Chlorocebus aethiops*, n=10; GSE103287 [32]) and in New World monkeys, from marmosets  
124 (*Callithrix jacchus*, n=6; GSE103287 [32]). From primates, only data from blood or femur was  
125 utilized. In addition to primates, we obtained DNA methylation data from guinea pig  
126 hippocampi (*Cavia porcellus*, n=36; GSE98549 [33]). As reference, we utilized data from  
127 human (*Homo sapiens*) blood (n=1658; GSE105018 [34]), femur (n=48; GSE64490 [35]) and  
128 hippocampus (n=33; GSE72778 [36]).

129 Methylation profiling data obtained by high throughput sequencing (guinea pigs, GSE98549)  
130 was processed as follows. Quality of the paired-end reads in all the samples was assessed using  
131 FastQC [37] and MultiQC [38]. Paired-end fastq files were trimmed using Trimmomatic-0.39  
132 with a sliding window of size 4 set to remove bases with phred score lower than 20 [39]. The  
133 trimmed samples were analyzed using Bismark-0.23.0 tools [40]. The reads were aligned to  
134 the guinea pig genome (cavPor3). Duplicate alignments, which can arise for example by PCR  
135 amplification, were removed. Methylation information was extracted from the alignment result  
136 files using Bismark's methylation extractor. DNA methylation values for CpGs inside the gene  
137 were first inspected and then a wider region ( $\pm 2000$ nt) around the gene was investigated.

138 Primate DNA methylation data from GSE41782, GSE105018, GSE64490, GSE72778  
139 (profiled with Illumina 450K) and GSE136296 (profiled with Illumina EPIC) were available  
140 as processed data and was used as such. Primate DNA methylation data from GSE103271,  
141 GSE103280, GSE103286, which are subseries of GSE103332 (profiled with Illumina EPIC),  
142 were available as raw data, and were normalized by using minfi quantile normalization for each  
143 species separately.

144 From primate data, the 14 CpGs in the *nc886* DMR previously reported to show bimodal  
145 methylation pattern in humans were retrieved [7,10]. In all the primate species, for which  
146 methylation data was available, the sequence on the binding site of the Illumina probes was  
147 investigated. Only data from sites with the CG-sequence intact in the species in question were  
148 further utilized. Also probes, which had mutations in the probe binding site and methylation  
149 pattern clearly distinct from neighboring sites, were discarded. Similar process was repeated  
150 for 50 probes in paternally expressed 10 (*PEG10*) previously shown to be imprinted [41].  
151 *PEG10* was used as evolutionally conserved reference for a classically imprinted gene [4].

152



## 153 **Results and Discussion**

### 154 ***nc886* gene in non-human mammals**

155 Human *nc886* has been suggested to be an evolutionally young gene, producing a 102 nt long  
156 RNA, which is then ineffectively cleaved to two miRNA-like RNAs [11]. In line with previous  
157 reports [7], *nc886* gene, with intact short RNA coding sequences and the hairpin loop, can be  
158 found in primates, in guinea pig (*Cavia porcellus*), Eurasian red squirrel (*Sciurus vulgaris*),  
159 and Alpine marmot (*Marmota marmota*), with two of the latter having insertions in the  
160 centromeric end of the gene (Figure 1, Supplementary figure S1).

161 Upon further inspection of primate *nc886* gene, almost 100% sequence similarity was identified  
162 in apes (*hominoidea*). The sequence similarity was high (over 98%) between humans and the  
163 investigated Old World monkeys (*Cercopithecidae*), while less (91-93%) similarity can be seen  
164 between humans and New World monkeys (*Ceboidea*) and even less (84-89%) between  
165 humans and tarsiers (*Tarsiidae*) or lemurs (*Lemuroidea*). Sequences coding for the short *nc886*  
166 RNAs are identical within Old World anthropoids (*Catarrhini*). Differences between human  
167 and New World monkey and prosimian *nc886* sequences can be found both in the short *nc886*  
168 RNA and the hairpin coding regions, but the most significant differences can be found in the  
169 centromeric end of the gene (Figure 1 and Supplementary figure S2).

170

### 171 **CTCF binding site sequence in mammals with *nc886* gene**

172 In humans, the *nc886* locus is flanked by two CTCF binding sites [7]. The telomeric CTCF  
173 binding site can be found in most vertebrates, with the binding sequence being identical in all  
174 species showed to have the *nc886* gene. The telomeric CTCF binding site was shown to interact  
175 with a CTCF binding site (chr5:135222814-135223707) locating near the *IL9* gene in the CTCF  
176 CiA-PET data. This prediction is in line with our previous finding indicating that genetic

177 polymorphisms near *IL9* gene are associated with the expression of *nc886* RNAs [10]. Together  
178 these results suggest that the evolutionally conserved telomeric CTCF binding site of *nc886*  
179 interacts with CTCF binding sites near *IL9* gene, possibly forming a topologically associating  
180 domain (TAD), or an interaction within one (sub-TAD), and bringing the suggested enhancer  
181 area near the *nc886* gene [42]. On the contrary, the centromeric CTCF binding site is present  
182 only in primates and even in primates, the binding sequence cannot be identified in marmosets.  
183 For the centromeric CTCF binding site no interactions were detected according to CTCF CiA-  
184 PET data. There are also changes in the CTCF binding sequence in gorillas (position 9), in all  
185 Old World monkeys (position 4) and also in New World monkeys (position 14). According to  
186 the CTCFBSDB 2.0, the guinea pig genome does not harbor any non-homologous predicted  
187 CTCF binding sites in the centromeric side of the *nc886* gene.

188

### 189 **Guinea pigs present a non-methylated *nc886* locus**

190 One of the aims of this study was to investigate whether the information gathered from the  
191 *nc886* gene and DMR from cell culture and population studies could be supplemented with  
192 research on animal models. In line with a previous report [7] we identified this gene only in  
193 primates, guinea pigs and few members of the squirrel family, of which guinea pig was the  
194 most promising candidate as a model organism. In data from Boureau et al. [33], in guinea pig  
195 hippocampi the whole *nc886/vtRNA2-1* gene was non-methylated (Supplementary figure S3A).  
196 The surrounding *nc886* region (Scaffold DS562872.1: 24,622,179-24,622,280) +/- 2000 nt was  
197 mostly unmethylated, with only 2% of the reads in the region being methylated. It should be  
198 noted that the number of reads in the region in the data utilized was low (max number of  
199 reads=17, average number of reads=7). *nc886* methylation pattern in human hippocampi  
200 presented the expected bimodal distribution, and thus the discovered methylation pattern in the

201 guinea pig hippocampi was most likely not due to the selection of tissue (Supplementary figure  
202 S3B). This identified lack of methylation in the *nc886* locus is compatible with the absence of  
203 the telomeric CTCF binding site, as CTCF binding sites can delineate the boundaries of an  
204 imprinted region [43]. These results thus suggest that guinea pigs are not suitable model  
205 organisms for the investigation of establishment of *nc886* methylation status.

206

### 207 **Imprinted *nc886* region in great apes**

208 The blood of chimpanzees, gorillas, bonobos and orangutans presented beta-values close to 0.5  
209 with a unimodal distribution in the *nc886* region (Figure 2). This methylation pattern closely  
210 resembles the methylation pattern in the known maternally imprinted gene *PEG10*  
211 (Supplementary figure S4). The methylation levels are also very similar to those presented in  
212 hemi-methylated humans (Figure 2). In these data sets, that include more than 110 apes, we  
213 did not identify any individuals with methylation level close to 0 in the *nc886* locus, whereas  
214 in humans 25% of the population present a methylation level close to 0 at this locus [7,10]. If  
215 the prevalence on non- and hemi-methylated individuals in apes was similar to humans, already  
216 11 individuals would present at least one non-methylated individual with 95% probability. Of  
217 individual species, we had the largest dataset for chimpanzees (n=83 in GSE13629631 and n=5  
218 in GSE41782). Again, assuming the same proportion of non-methylated individuals as in  
219 humans (25%), probability of not identifying any non-methylated chimpanzees in a population  
220 of 88 individuals is extremely low,  $1.01 \cdot 10^{-11}$ . These results imply that the *nc886* locus is not  
221 polymorphically imprinted in apes.

222 Within species standard deviation of the methylation in a probe is on average around 0.04,  
223 which is comparable to that seen in *PEG10* in apes (SD on average 0.04) and in human blood  
224 (0.02), indicating good data quality. In all apes the methylation levels of *nc886* region

225 resembled those seen in *PEG10*, which is an evolutionally conserved maternally imprinted  
226 gene [4]. It is thus reasonable to suggest that *nc886* could be classically imprinted in other great  
227 apes, excluding humans.

228

### 229 ***nc886* region methylation patterns in Old World monkeys**

230 The patterns of *nc886* region methylation are very similar in all of the Old World monkeys.  
231 The median methylation level is close to 0.60, higher as compared to apes. The interindividual  
232 variation is larger, especially in baboons, than in apes, with the average SD within a probe  
233 being 0.11. The SD within a probe is also higher in probes locating in *PEG10* in baboons,  
234 where the within probe SD is on average 0.07. As the between individual variation in  
235 methylation levels of a known evolutionally conserved imprinted gene is also higher, this  
236 suggests a technical bias in the data, potentially due to the use of Illumina Infinium 450K and  
237 EPIC methylation assays, that are designed for humans. All methylation data available for Old  
238 World monkeys was from femur, but as in the human reference data set from femur samples  
239 both *nc886* and *PEG10* present similar methylation patterns as in blood (Figure 3 and  
240 Supplementary figure S5), this phenomenon most likely is not caused by the tissue of origin.  
241 Regardless of the precise methylation levels of the Old World monkeys, in the 48 individuals  
242 we did not identify any presenting a non-methylated methylation pattern in *nc886* region,  
243 probability of which is  $1.0 \cdot 10^{-6}$ , when assuming similar distribution as in humans. This implies  
244 that similar to non-human great apes, the *nc886* locus is not polymorphically imprinted in Old  
245 World monkeys.

246

### 247 ***nc886* region methylation patterns in New World monkeys**

248 Data from the six marmosets is not conclusive, as we found that only 3 of the probes in *nc886*  
249 region bound to areas with no great sequence differences. The methylation levels of two of  
250 these probes were around 0.8 and one 0.32, showing no indications of imprinting, while the  
251 methylation beta values in the probes locating in the *PEG10* are on average 0.48 in marmosets  
252 (Figure 3 and Supplementary figure S5). The lack of imprinting of any kind in marmosets is  
253 further supported by the finding that they lack the centromeric CTCF binding sequence, which  
254 is thought to have an important role in insulating the DMR [7].

255

### 256 **Limitations of the study**

257 Our study is purely descriptive in nature. In guinea pigs, the shallowness of the sequencing  
258 data limits the ability to make conclusions of the methylation pattern. In non-human primates,  
259 utilizing methylation arrays that have been designed for humans raises questions on data  
260 quality, especially in marmosets. Concerns over data quality are however mitigated by the  
261 observed methylation pattern in well-established imprinted gene, *PEG10*, as well as the  
262 consistency of observed results across different species and data sets.

263

### 264 **Conclusions**

265 We describe here an analysis on the methylation status of *nc886* region in non-human  
266 mammals. A genetic locus, with more than 80% similarity to human *nc886* gene can be found  
267 in primates, guinea pigs and some members of the squirrel family. We obtained DNA  
268 methylation data for 8 different non-human primate species and for guinea pigs, and in none  
269 of these species could we observe methylation pattern indicative of similar polymorphic  
270 imprinting, as could be observed, and has been reported [7,9,10], in humans. The observed  
271 methylation pattern in apes and in Old World monkeys implies that the *nc886* region might be

272 classically imprinted, although these findings have to be interpreted with caution, as apart from  
273 chimpanzees the sample number were low, and in Old World monkeys the variation between  
274 individuals was notable. In guinea pigs, the most feasible potential model organism of those  
275 harboring the *nc886* locus, the data indicated that the locus is completely unmethylated. It is  
276 noteworthy that only primates, whose genome also contained the centromeric CTCF binding  
277 sequence flanking the *nc886* gene, had methylation levels indicative of genetic imprinting.

278 As such, it appears there are no animal models suited to study the establishment of the  
279 methylation pattern of the polymorphically imprinted metastable epiallele *nc886*. Further  
280 studies on how this kind of unusual metastable developed, and how it links to the  
281 periconceptual conditions and later life health traits, are thus restricted to *in vitro* and  
282 population studies.

283

## 284 **Declarations**

## 285 **Ethics approval:**

286 Datasets used in this study were retrieved from Gene Expression Omnibus (GEO,  
287 [www.ncbi.nlm.nih.gov/geo/](http://www.ncbi.nlm.nih.gov/geo/)) repository. For human data sets, informed consent or “Consent  
288 for Autopsy” were given by all participants. For animal studies all protocols were approved by  
289 the local ethical committees and/or the samples were collected during standard veterinary  
290 checks or routine necropsies. Details can be found from the original publications[30–36].

291 **Consent for publication:** Not applicable

292 **Availability of data and materials:** All methylation data utilized is available in GEO, under  
293 accession numbers GSE136296, GSE41782, GSE103287, GSE98549, GSE105018,  
294 GSE64490 and GSE72778.

295 **Competing interests:** The authors declare that they have no competing interests

296 **Funding:** This study has been supported by the Academy of Finland (grants 330809 and  
297 338395 (E.R.)); the Tampere University Hospital Medical Funds (grants 9X047, 9S054, and  
298 9AB059 for E.R.); the Yrjö Jahnsson Foundation (S.M. and E.R.); the Foundation of Clinical  
299 Chemistry (E.R), Laboratoriolääketieteen edistämistätiö sr. (E.R.) and the Paulo Foundation  
300 (S.M).

301 **Author Contributions:** S.M. and E.R. designed the research; D.K., H.T., P.P.M., S.M. and  
302 E.R. performed research; S.M. and E.R. provided resources; D.K., H.T., P.P.M., S.M. and E.R.  
303 curated data; S.M. and E.R wrote the original draft manuscript; D.K., H.T., P.P.M., S.M. and  
304 E.R. reviewed and edited the manuscript. Funding was acquired by S.M and E.R. All authors  
305 have read and agreed upon the published version of the manuscript.

306 **Acknowledgements:** The authors wish to thank Jooseppi Järvinen (MSc) for his contribution  
307 to the probability calculations, Nina Mononen (PhD) and Binisha Mishra (MSc) for their  
308 valuable input on the manuscript and to acknowledge all the researchers who contributed  
309 towards the collection of datasets utilized in this study.

## 310 **References:**

- 311 1. Smith FM, Garfield AS, Ward A. Regulation of growth and metabolism by imprinted  
312 genes. *Cytogenetic and Genome Research*. 2006. doi:10.1159/000090843
- 313 2. Millership SJ, Van de Pette M, Withers DJ. Genomic imprinting and its effects on  
314 postnatal growth and adult metabolism. *Cellular and Molecular Life Sciences*. 2019.  
315 doi:10.1007/s00018-019-03197-z
- 316 3. Barlow DP, Bartolomei MS. Genomic imprinting in mammals. *Cold Spring Harbor*  
317 *Perspectives in Biology*. 2014;6. doi:10.1101/cshperspect.a018382

- 318 4. Renfree MB, Suzuki S, Kaneko-Ishino T. The origin and evolution of genomic  
319 imprinting and viviparity in mammals. *Philosophical Transactions of the Royal*  
320 *Society B: Biological Sciences*. 2013. doi:10.1098/rstb.2012.0151
- 321 5. Varmuza S, Mann M. Genomic imprinting - defusing the ovarian time bomb. *Trends in*  
322 *Genetics*. 1994;10. doi:10.1016/0168-9525(94)90212-7
- 323 6. Lewis A, Reik W. How imprinting centres work. *Cytogenetic and Genome Research*.  
324 2006. doi:10.1159/000090818
- 325 7. Carpenter BL, Zhou W, Madaj Z, DeWitt AK, Ross JP, Grønbaek K, et al. Mother-  
326 child transmission of epigenetic information by tunable polymorphic imprinting.  
327 *Proceedings of the National Academy of Sciences of the United States of America*.  
328 2018. doi:10.1073/pnas.1815005115
- 329 8. Silver MJ, Kessler NJ, Hennig BJ, Dominguez-Salas P, Laritsky E, Baker MS, et al.  
330 Independent genomewide screens identify the tumor suppressor VTRNA2-1 as a  
331 human epiallele responsive to periconceptual environment. *Genome Biology*. 2015.  
332 doi:10.1186/s13059-015-0660-y
- 333 9. Carpenter BL, Remba TK, Thomas SL, Madaj Z, Brink L, Tiedemann RL, et al.  
334 Oocyte age and preconceptual alcohol use are highly correlated with  
335 epigenetic imprinting of a noncoding RNA (nc886). *Proceedings of the National*  
336 *Academy of Sciences of the United States of America*. 2021;118.  
337 doi:10.1073/pnas.2026580118
- 338 10. Marttila S, Viiri LE, Mishra PP, Kühnel B, Matias-Garcia PR, Lyytikäinen L-P, et al.  
339 Methylation status of nc886 epiallele reflects periconceptual conditions and is  
340 associated with glucose metabolism through nc886 RNAs. *Clinical Epigenetics*.  
341 2021;13. doi:10.1186/s13148-021-01132-3



- 342 11. Fort RS, Garat B, Sotelo-Silveira JR, Duhagon MA. vtRNA2-1/nc886 produces a  
343 small RNA that contributes to its tumor suppression action through the microRNA  
344 pathway in prostate cancer. *Non-coding RNA*. 2020. doi:10.3390/ncrna6010007
- 345 12. Kong L, Hao Q, Wang Y, Zhou P, Zou B, Zhang Y xiang. Regulation of p53  
346 expression and apoptosis by vault RNA2-1-5p in cervical cancer cells. *Oncotarget*.  
347 2015. doi:10.18632/oncotarget.4948
- 348 13. Lee K, Kunkeaw N, Jeon SH, Lee I, Johnson BH, Kang GY, et al. Precursor miR-886,  
349 a novel noncoding RNA repressed in cancer, associates with PKR and modulates its  
350 activity. *RNA*. 2011. doi:10.1261/rna.2701111
- 351 14. Lee YS. A Novel Type of Non-coding RNA, nc886, Implicated in Tumor Sensing and  
352 Suppression. *Genomics & Informatics*. 2015. doi:10.5808/gi.2015.13.2.26
- 353 15. Steegers-Theunissen RPM, Twigt J, Pestinger V, Sinclair KD. The periconceptual  
354 period, reproduction and long-term health of offspring: The importance of one-carbon  
355 metabolism. *Human Reproduction Update*. 2013. doi:10.1093/humupd/dmt041
- 356 16. Gonseth S, Shaw GM, Roy R, Segal MR, Asrani K, Rine J, et al. Epigenomic profiling  
357 of newborns with isolated orofacial clefts reveals widespread DNA methylation  
358 changes and implicates metastable epiallele regions in disease risk. *Epigenetics*. 2019.  
359 doi:10.1080/15592294.2019.1581591
- 360 17. van Dijk SJ, Peters TJ, Buckley M, Zhou J, Jones PA, Gibson RA, et al. DNA  
361 methylation in blood from neonatal screening cards and the association with BMI and  
362 insulin sensitivity in early childhood. *International Journal of Obesity*. 2018.  
363 doi:10.1038/ijo.2017.228

- 364 18. Yu S, Zhang R, Liu G, Yan Z, Hu H, Yu S, et al. Microarray analysis of differentially  
365 expressed microRNAs in allergic rhinitis. *American Journal of Rhinology and Allergy*.  
366 2011. doi:10.2500/ajra.2011.25.3682
- 367 19. Suojalehto H, Lindström I, Majuri ML, Mitts C, Karjalainen J, Wolff H, et al. Altered  
368 microRNA expression of nasal mucosa in long-term asthma and allergic rhinitis.  
369 *International Archives of Allergy and Immunology*. 2014. doi:10.1159/000358486
- 370 20. Sharbati J, Lewin A, Kutz-Lohroff B, Kamal E, Einspanier R, Sharbati S. Integrated  
371 microrna-mrna-analysis of human monocyte derived macrophages upon  
372 mycobacterium avium subsp. hominissuis infection. *PLoS ONE*. 2011.  
373 doi:10.1371/journal.pone.0020258
- 374 21. Asaoka T, Sotolongo B, Island ER, Tryphonopoulos P, Selvaggi G, Moon J, et al.  
375 MicroRNA signature of intestinal acute cellular rejection in formalin-fixed paraffin-  
376 embedded mucosal biopsies. *American Journal of Transplantation*. 2012.  
377 doi:10.1111/j.1600-6143.2011.03807.x
- 378 22. Lin CH, Lee YS, Huang YY, Tsai CN. Methylation status of vault rna 2-1 promoter is  
379 a predictor of glycemic response to glucagon-like peptide-1 analog therapy in type 2  
380 diabetes mellitus. *BMJ Open Diabetes Research and Care*. 2021;9.  
381 doi:10.1136/bmjdr-2020-001416
- 382 23. Barker DJP, Osmond C. INFANT MORTALITY, CHILDHOOD NUTRITION, AND  
383 ISCHAEMIC HEART DISEASE IN ENGLAND AND WALES. *The Lancet*. 1986.  
384 doi:10.1016/S0140-6736(86)91340-1
- 385 24. Romanelli V, Nakabayashi K, Vizoso M, Moran S, Iglesias-Platas I, Sugahara N, et al.  
386 Variable maternal methylation overlapping the nc886/vtRNA2-1 locus is locked

- 387 between hypermethylated repeats and is frequently altered in cancer. *Epigenetics*.  
388 2014. doi:10.4161/epi.28323
- 389 25. Kent WJ, Sugnet CW, Furey TS, Roskin KM, Pringle TH, Zahler AM, et al. The  
390 Human Genome Browser at UCSC. *Genome Research*. 2002;12.  
391 doi:10.1101/gr.229102
- 392 26. Bou-Nader C, Gordon JM, Henderson FE, Zhang J. The search for a PKR code—  
393 differential regulation of protein kinase R activity by diverse RNA and protein  
394 regulators. *RNA*. 2019. doi:10.1261/rna.070169.118
- 395 27. Ziebarth JD, Bhattacharya A, Cui Y. CTCFBSDB 2.0: A database for CTCF-binding  
396 sites and genome organization. *Nucleic Acids Research*. 2013;41.  
397 doi:10.1093/nar/gks1165
- 398 28. Rosenbloom KR, Sloan CA, Malladi VS, Dreszer TR, Learned K, Kirkup VM, et al.  
399 ENCODE Data in the UCSC Genome Browser: Year 5 update. *Nucleic Acids*  
400 *Research*. 2013;41. doi:10.1093/nar/gks1172
- 401 29. Barrett T, Wilhite SE, Ledoux P, Evangelista C, Kim IF, Tomashevsky M, et al. NCBI  
402 GEO: Archive for functional genomics data sets - Update. *Nucleic Acids Research*.  
403 2013;41. doi:10.1093/nar/gks1193
- 404 30. Guevara EE, Lawler RR, Staes N, White CM, Sherwood CC, Ely JJ, et al. Age-  
405 associated epigenetic change in chimpanzees and humans. *Philosophical Transactions*  
406 *of the Royal Society B: Biological Sciences*. 2020;375. doi:10.1098/rstb.2019.0616
- 407 31. Hernando-Herraez I, Prado-Martinez J, Garg P, Fernandez-Callejo M, Heyn H,  
408 Hvilsom C, et al. Dynamics of DNA Methylation in Recent Human and Great Ape  
409 Evolution. *PLoS Genetics*. 2013;9. doi:10.1371/journal.pgen.1003763

- 410 32. Housman G, Quillen EE, Stone AC. Intraspecific and interspecific investigations of  
411 skeletal DNA methylation and femur morphology in primates. *American Journal of*  
412 *Physical Anthropology*. 2020;173. doi:10.1002/ajpa.24041
- 413 33. Boureau L, Constantinof A, Moisiadis VG, Matthews SG, Szyf M. The DNA  
414 methylation landscape of enhancers in the Guinea pig hippocampus. *Epigenomics*.  
415 2018;10. doi:10.2217/epi-2017-0064
- 416 34. Hannon E, Knox O, Sugden K, Burrage J, Wong CCY, Belsky DW, et al.  
417 Characterizing genetic and environmental influences on variable DNA methylation  
418 using monozygotic and dizygotic twins. *PLoS Genetics*. 2018.  
419 doi:10.1371/journal.pgen.1007544
- 420 35. Horvath S, Mah V, Lu AT, Woo JS, Choi OW, Jasinska AJ, et al. The cerebellum ages  
421 slowly according to the epigenetic clock. *Aging*. 2015;7. doi:10.18632/aging.100742
- 422 36. Horvath S, Langfelder P, Kwak S, Aaronson J, Rosinski J, Vogt TF, et al.  
423 Huntington's disease accelerates epigenetic aging of human brain and disrupts DNA  
424 methylation levels. *Aging*. 2016;8. doi:10.18632/aging.101005
- 425 37. Andrews S. FastQC - A quality control tool for high throughput sequence data.  
426 <http://www.bioinformatics.babraham.ac.uk/projects/fastqc/>. Babraham Bioinformatics.  
427 2010.
- 428 38. Ewels P, Magnusson M, Lundin S, Källér M. MultiQC: Summarize analysis results for  
429 multiple tools and samples in a single report. *Bioinformatics*. 2016;32.  
430 doi:10.1093/bioinformatics/btw354
- 431 39. Bolger AM, Lohse M, Usadel B. Trimmomatic: A flexible trimmer for Illumina  
432 sequence data. *Bioinformatics*. 2014;30. doi:10.1093/bioinformatics/btu170

- 433 40. Krueger F, Andrews SR. Bismark: A flexible aligner and methylation caller for  
434 Bisulfite-Seq applications. *Bioinformatics*. 2011;27. doi:10.1093/bioinformatics/btr167
- 435 41. Hernandez Mora JR, Tayama C, Sánchez-Delgado M, Monteagudo-Sánchez A, Hata  
436 K, Ogata T, et al. Characterization of parent-of-origin methylation using the Illumina  
437 Infinium MethylationEPIC array platform. *Epigenomics*. 2018;10. doi:10.2217/epi-  
438 2017-0172
- 439 42. Kentepozidou E, Aitken SJ, Feig C, Stefflova K, Ibarra-Soria X, Odom DT, et al.  
440 Clustered CTCF binding is an evolutionary mechanism to maintain topologically  
441 associating domains. *Genome Biology*. 2020;21. doi:10.1186/s13059-019-1894-x
- 442 43. Downen JM, Fan ZP, Hnisz D, Ren G, Abraham BJ, Zhang LN, et al. Control of cell  
443 identity genes occurs in insulated neighborhoods in mammalian chromosomes. *Cell*.  
444 2014;159. doi:10.1016/j.cell.2014.09.030
- 445
- 446

447 **Figure legends**

448 **Figure 1.** Schematic presentation of the similarity of the *nc886* gene and flanking CTCF  
449 binding sites. Sequence similarity decreases with the diluting color intensity. Guinea pigs lack  
450 the whole centromeric flanking CTCF binding site, whilst the marmosets have a region with  
451 sequence similarity, but lack the binding sequence of the CTCF. For detailed sequence  
452 comparisons, see Supplementary figures S1 and S2.

453

454 **Figure 2.** Blood DNA methylation beta values in *nc886* region in great apes (*Hominidae*). In  
455 each graph, one dot represents one individual. In humans a bimodal methylation pattern can  
456 be detected, in line with the expected population distribution of hemi-methylated (75% of the  
457 population, methylation level ~0.5) and non-methylated individuals (25% of the population,  
458 methylation level close to 0 [10]). All of the other species present a unimodal methylation  
459 pattern, with all individual having methylation beta-values near 0.5 across the *nc886* locus.

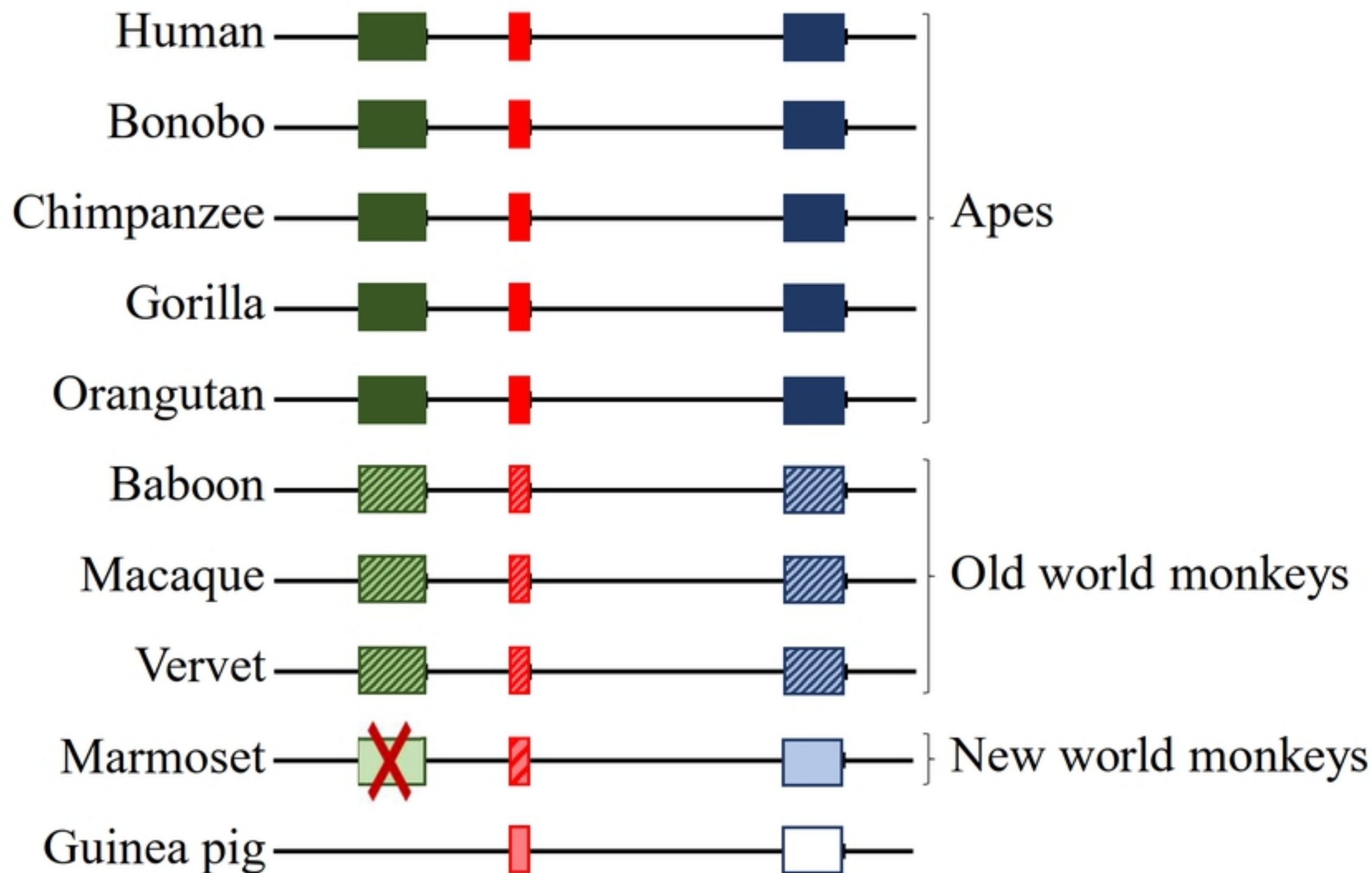
460

461 **Figure 3.** Femur DNA methylation beta values in the *nc886* region in humans and in monkeys.  
462 In humans a bimodal methylation pattern can be detected, similar to blood and in line with  
463 expected population distribution of non- and hemi-methylated individuals [10]. In Old World  
464 monkeys the between individual variation is bigger than in apes. No individuals presenting a  
465 non-methylated *nc886* region are detected. In marmosets only 3 probes were considered to  
466 provide reliable methylation values and none of them present methylation levels near 0.5.

467

468 **Supplementary files**

469 Supplementary file 1 (.docx) containing Supplementary Figures S1-S5 with captions.

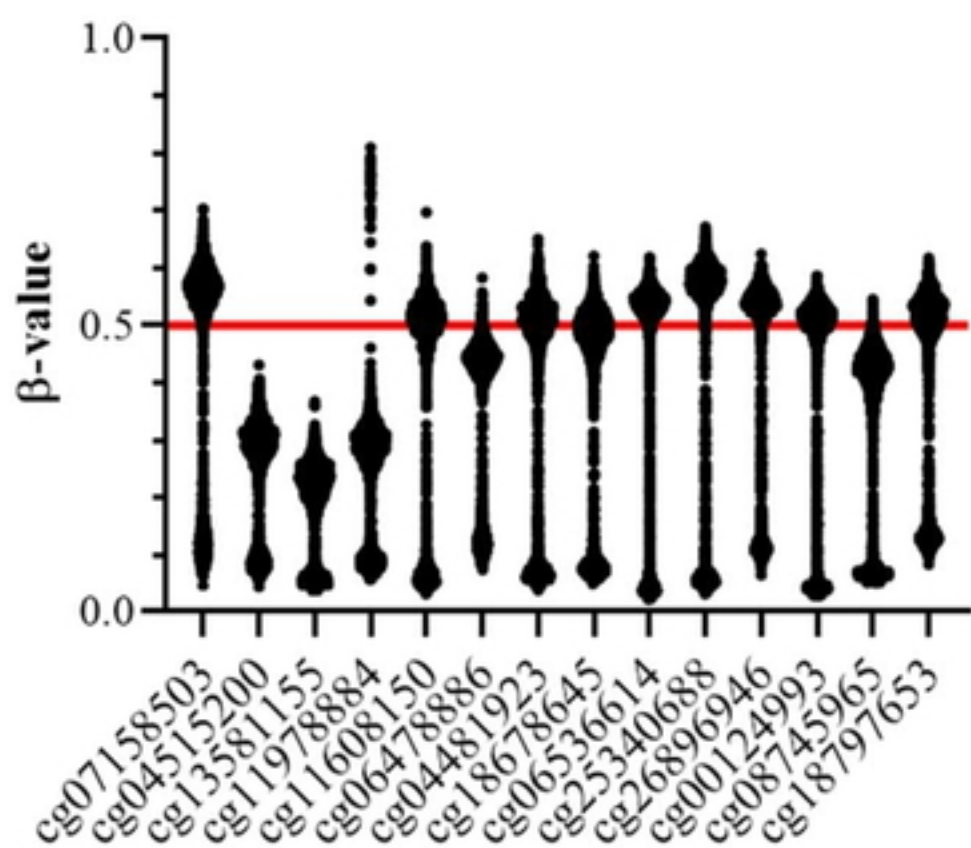


- Centromeric CTCF binding site
- nc886* gene
- Telomeric CTCF binding site
- Centromeric CTCF binding site lacking the CTCF binding sequence

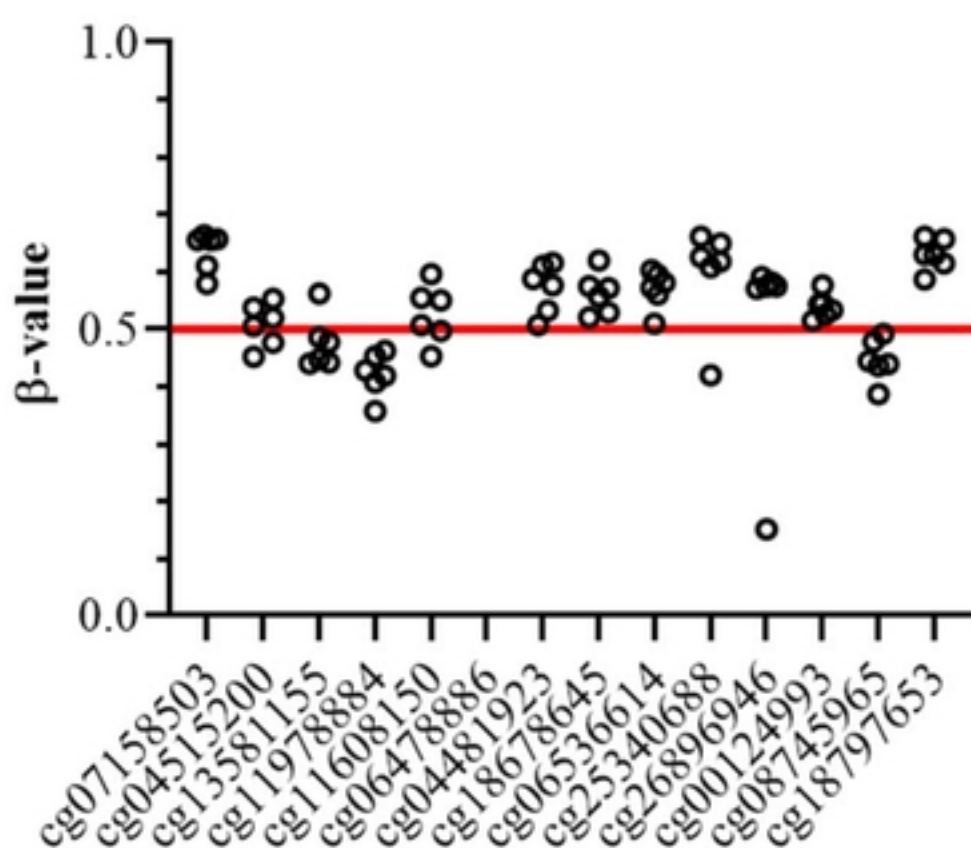
Figure 1



**nc886 Human blood  
GSE105018**

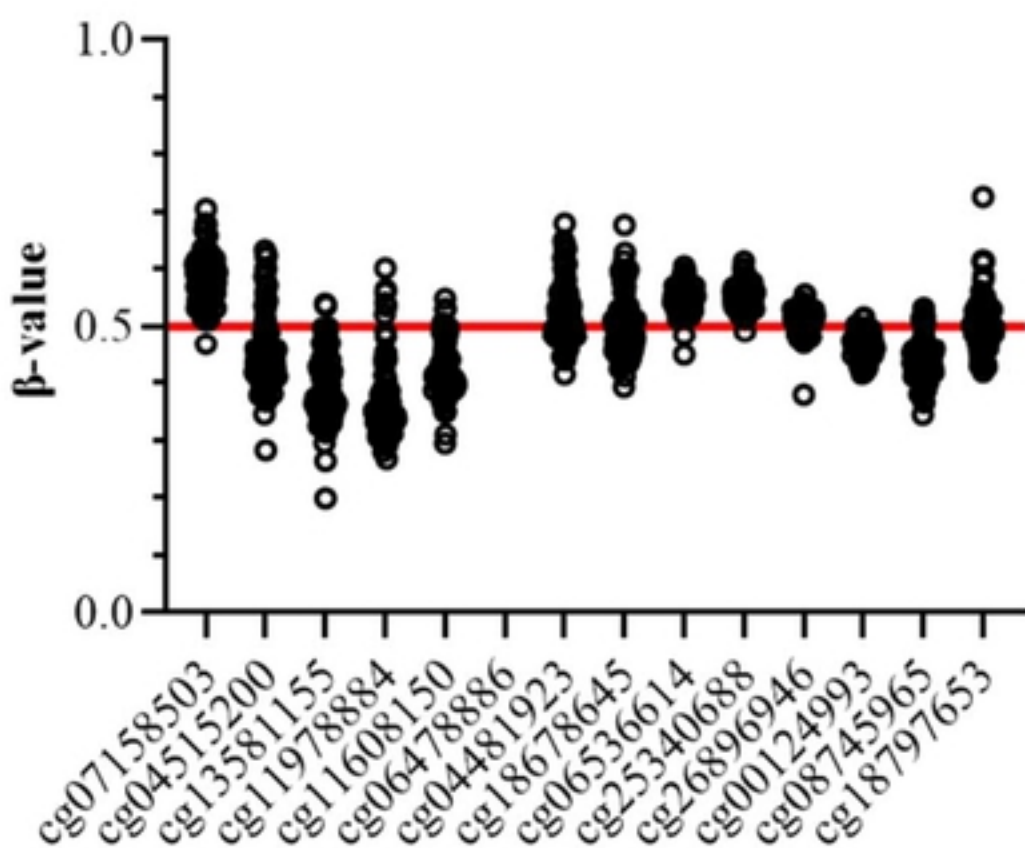


**nc886 Bonobo blood  
GSE41782**

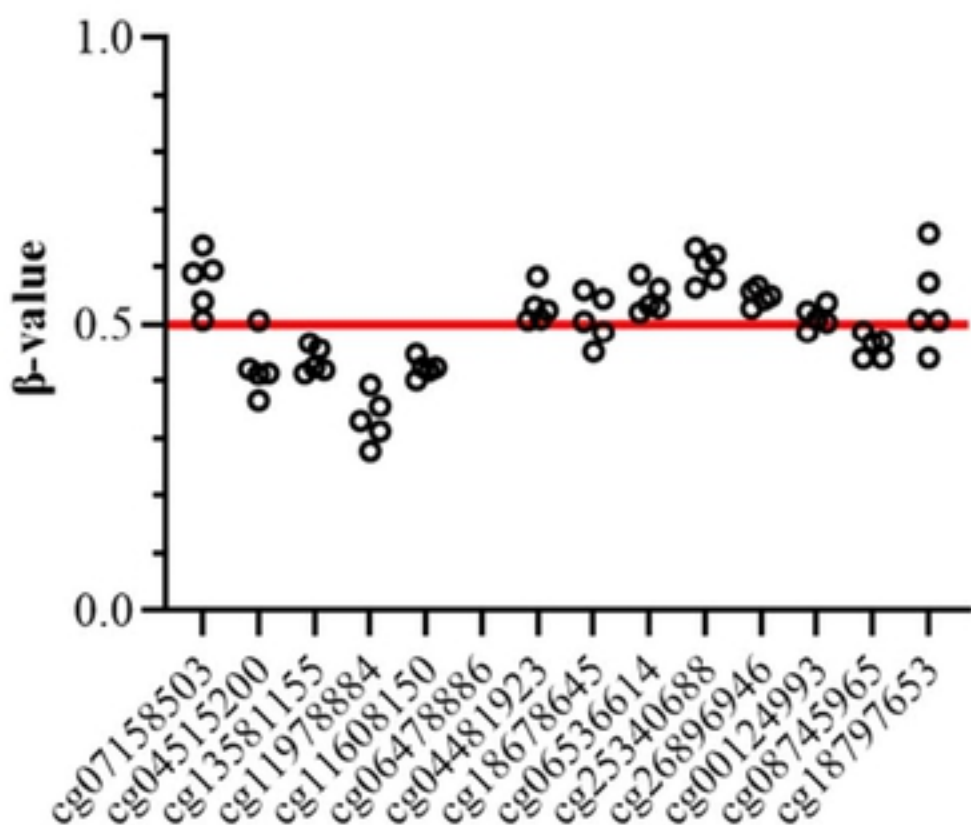


bioRxiv preprint doi: <https://doi.org/10.1101/2021.12.03.471165>; this version posted December 3, 2021. The copyright holder for this preprint (which was not certified by peer review) is the author/funder, who has granted bioRxiv a license to display the preprint in perpetuity. It is made available under aCC-BY 4.0 International license.

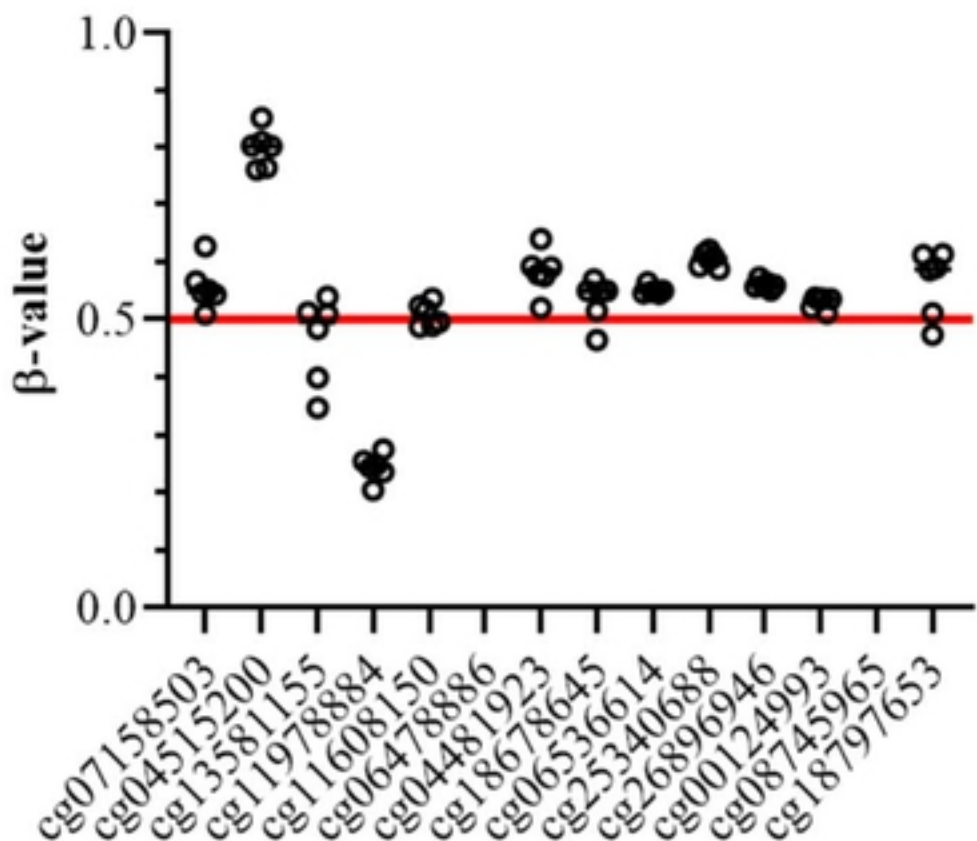
**nc886 Chimpanzee blood  
GSE136296**



**nc886 Chimpanzee blood  
GSE41782**



**nc886 Gorilla blood  
GSE41782**



**nc886 Orangutan blood  
GSE41782**

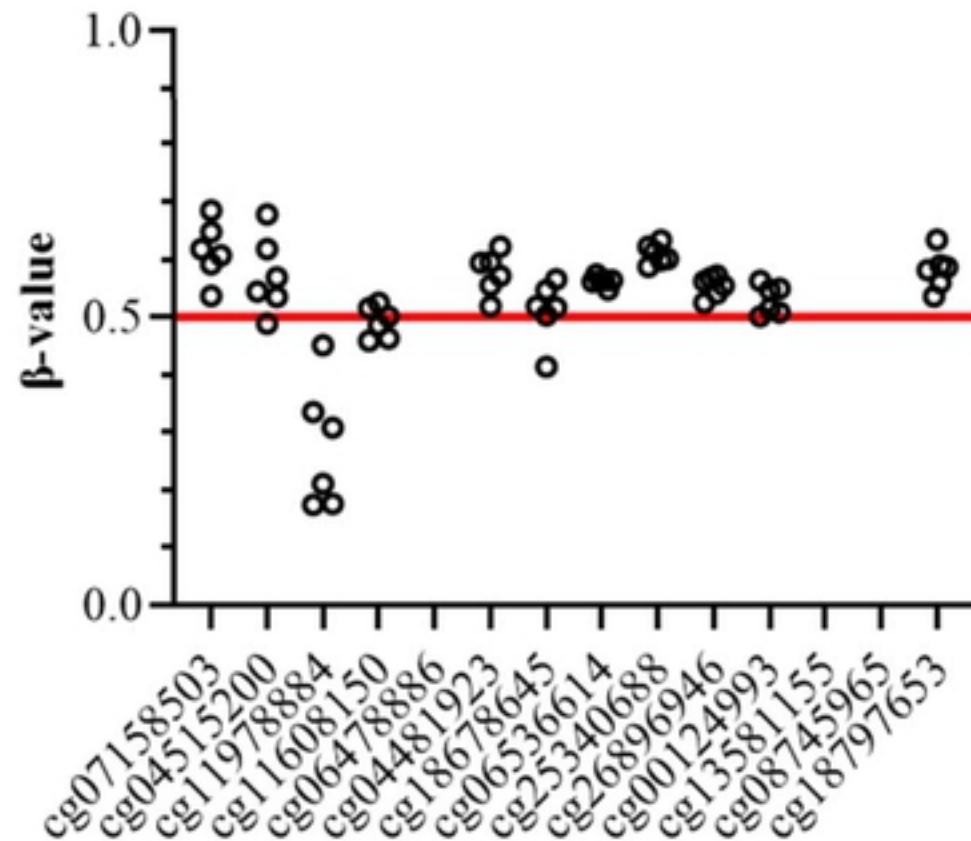
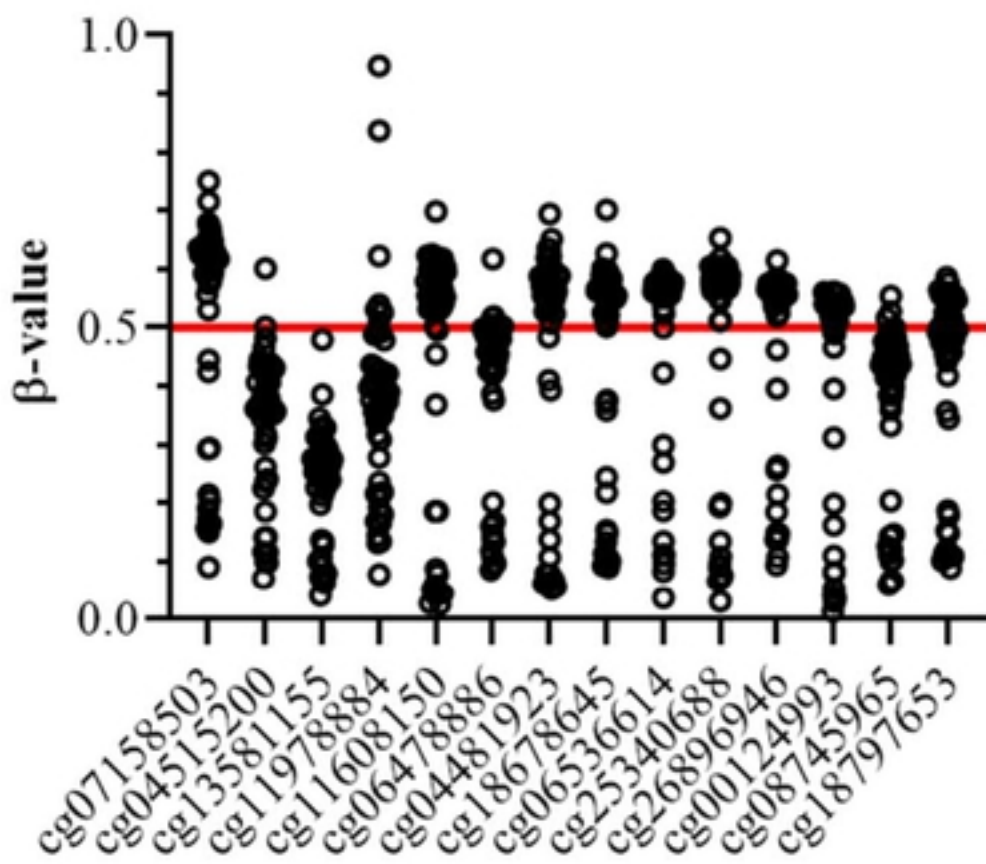


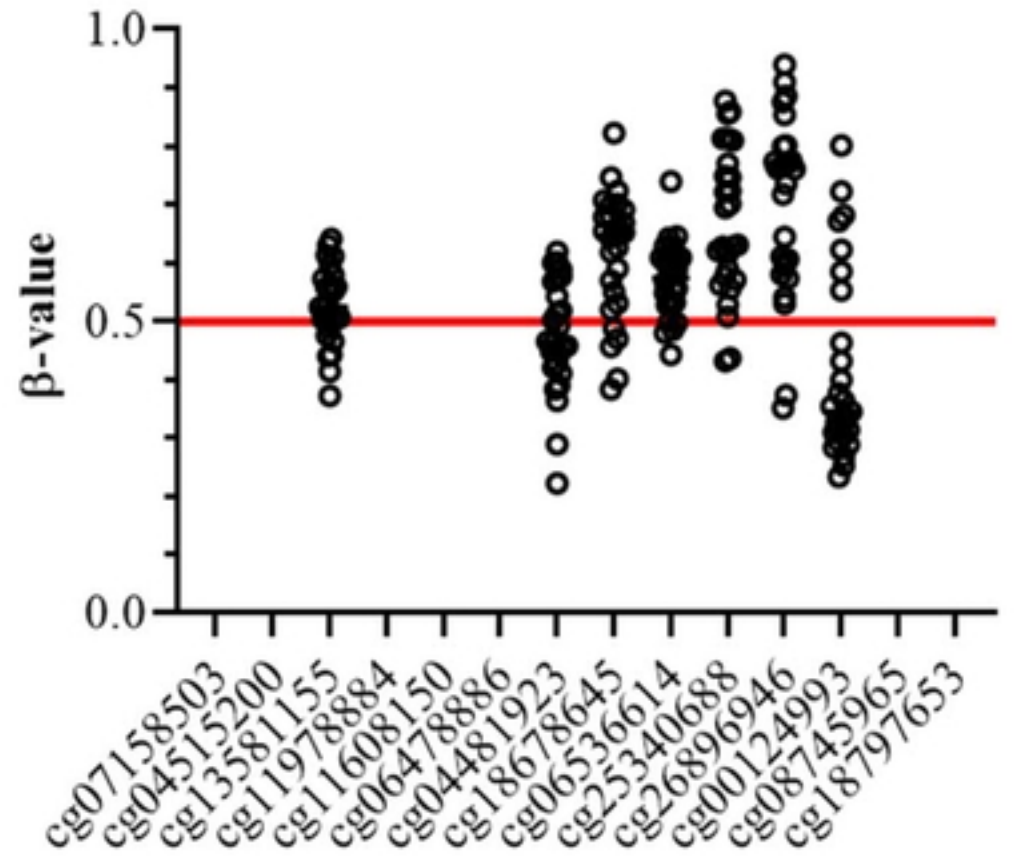
Figure 2



**nc886 Human femur  
GSE64490**

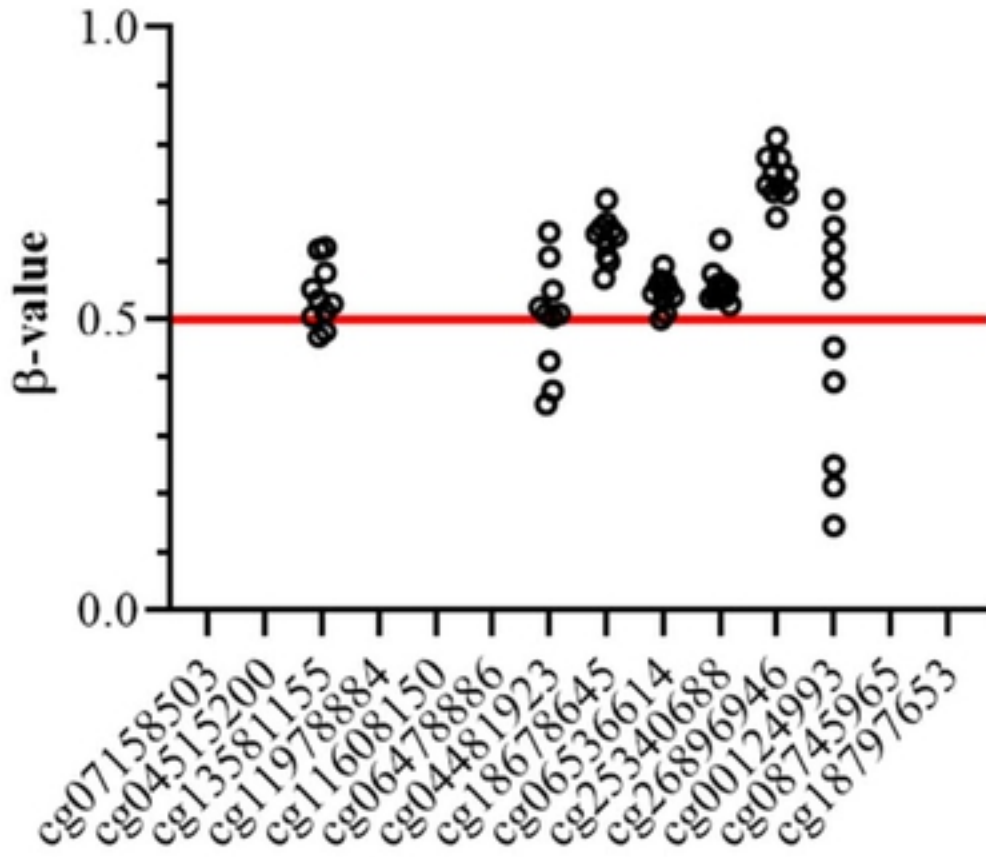


**nc886 Baboon femur  
GSE103286**

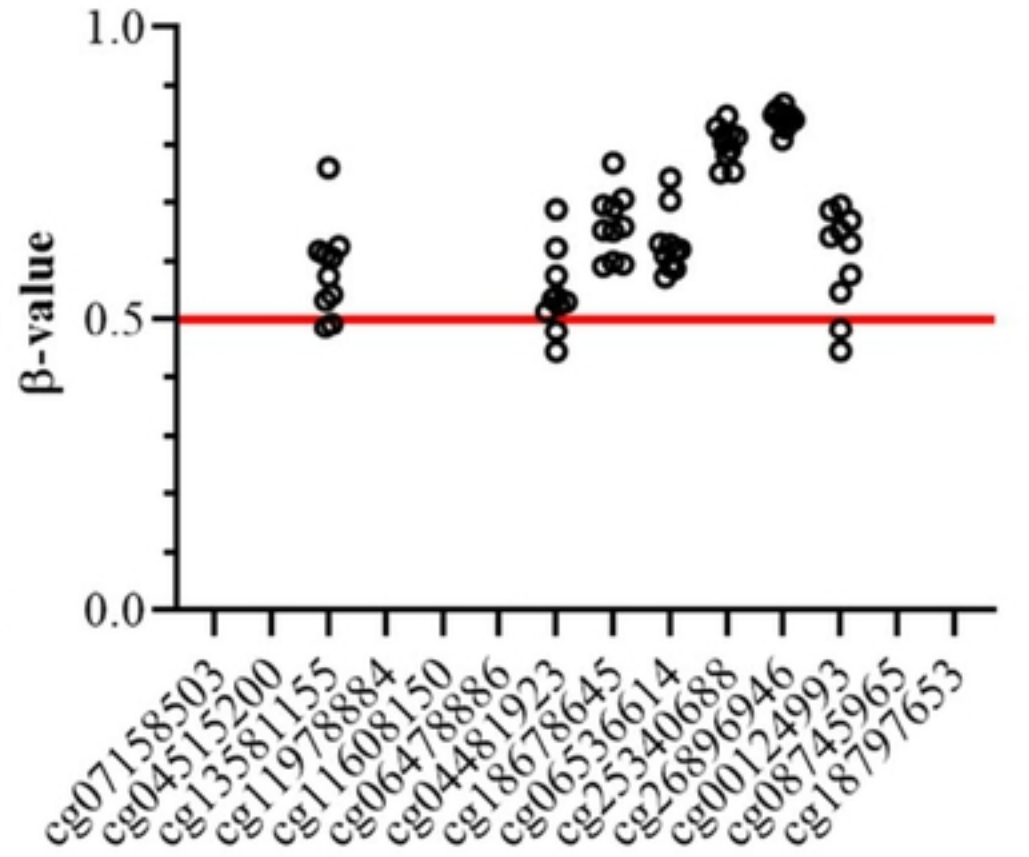


bioRxiv preprint doi: <https://doi.org/10.1101/2021.12.03.471165>; this version posted December 3, 2021. The copyright holder for this preprint (which was not certified by peer review) is the author/funder, who has granted bioRxiv a license to display the preprint in perpetuity. It is made available under aCC-BY 4.0 International license.

**nc886 Macaque femur  
GSE52944**



**nc886 Vervet femur  
GSE103280**



**nc886 Marmoset femur  
GSE103328**

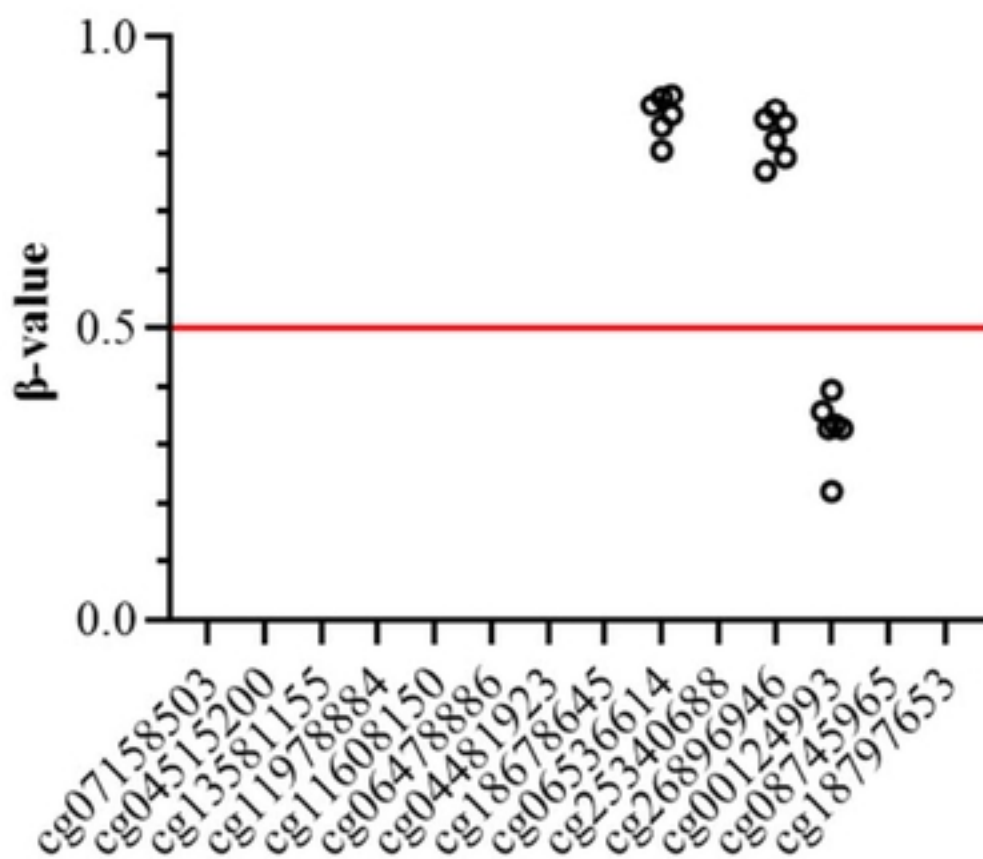


Figure 3